

Hybrid distributed & decentralized secondary control strategy to attain accurate power sharing and improved voltage restoration in dc microgrids

Waner Wodson A. G. Silva, *Student Member, IEEE*, Thiago R. Oliveira, *Member, IEEE*, and Pedro F. Donoso-Garcia

Abstract—This paper proposes a secondary level control technique for dc microgrids, which achieves accurate power sharing through a distributed strategy whilst performing dc bus voltage restoration in a decentralized fashion. In order to attain proper power sharing, each power converter exchanges its output power information with neighboring converters through a low-bandwidth network at defined time intervals. A consensus-based algorithm is employed to process this information and modify the converter’s droop coefficient, compensating droop mismatches and cable resistances and enabling power sharing. Restoration of the average dc bus voltage is realized locally with each converter compensating its own output voltage drop through an integrator. A comprehensive design procedure and performance and stability analysis, including communication loss and substantial time delays are also provided. The strategy has shown to be robust to some communication failure scenarios and moderate communication delays. The proposed method is evaluated through PLECS simulation and it is experimentally validated in a 4.5 kW dc microgrid setup.

Index Terms—Dc microgrids, accurate power sharing, voltage restoration, consensus-based algorithm, droop-control.

I. INTRODUCTION

THE microgrid concept was introduced as a solution for the integration of multiple power sources and storage systems into the grid, where those resources are conjugated in a local power system, enabling optimal usage of distributed generation, power dispatch and autonomous operation [1], [2]. DC microgrids are a growing subject in this field, since they provide simplified power control, due to the lack of reactive power flow, phase synchronization and ac power quality issues [3], as well as a more efficient integration with distributed generation and storage, due to the elimination of unnecessary power conversion stages [4], [5]. Fig. 1 presents a typical residential level dc microgrid and its main elements: a Bidirectional Interface Converter (BIC), responsible for interconnecting the microgrid and the utility grid at the point of common coupling (PCC), a Renewable Resource Interface Converter (RRC), which interconnects the distributed generation to the microgrid main dc bus and an Energy Storage Interface Converter (ESC). ESC is responsible for ensuring the power balance either in on-grid or in island operation. The backbone of the dc microgrid is a 380V dc bus, which interlinks all converters and supplies local dc loads.

Waner Wodson A. G. da Silva is with the Federal University of Itajuba (UNIFEI), Itabira, Brazil, e-mail: waner@unifei.edu.br.

Thiago R. Oliveira is with Electronic Engineering Department, Federal University of Minas Gerais (UFMG), Belo Horizonte, Brazil, e-mail: troliveira@cpdee.ufmg.br

Pedro F. Donoso-Garcia is with the Electronic Engineering Department, Federal University of Minas Gerais (UFMG), Belo Horizonte, Brazil, e-mail: pedro@cpdee.ufmg.br

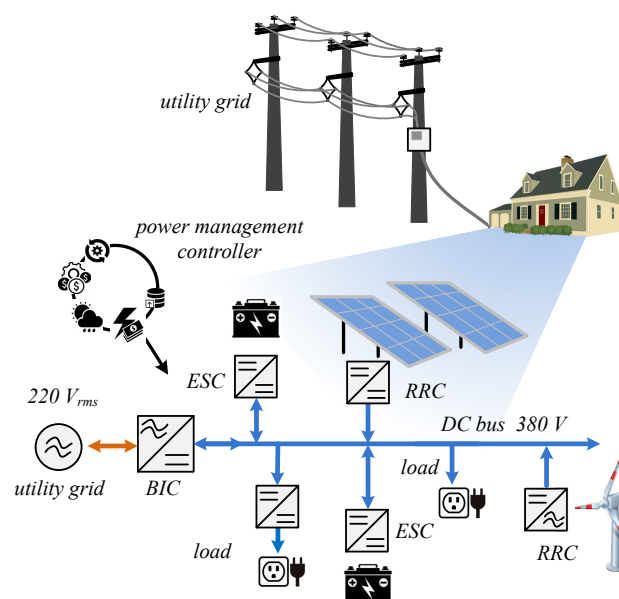


Fig. 1. Residential dc microgrid

The power management of dc microgrids is usually based on a hierarchical structure, adapted from ISA-95 standards, which considers three control layers:

- **Primary control:** this level refers to the local control of the power converters. It is responsible to ensure power sharing and dc bus voltage regulation and stability [2], [4], [5]. The control techniques employed in this layer mostly consist of i) centralized control, based on high or low bandwidth links, in which a central element determines the operation mode of all microgrid converters, either by defining one to be in voltage mode and regulate the dc bus voltage whereas the others operate as current sources, or by defining the current references of each converter in a master-slave approach [6], [7], [8], [9]; ii) droop-control, a decentralized approach in which each converter voltage reference is dependent on its output power [10]–[12];
- **Secondary control:** this layer is responsible for compensating the errors introduced by the primary control [2];
- **Tertiary control:** this layer manages the power flow between the microgrid and the utility network. It can establish voltage and current references at the PCC and modify primary control parameters depending on economic and environmental data, in order to achieve optimized operation of the microgrid [2], [13].

Droop control in the primary level provides high reliability and flexibility to the microgrid, since proper power sharing

and stable operation of paralleled converters are guaranteed without the need for a communication network, which also intrinsically introduces plug-and-play capability to it. Consequently, droop controlled microgrids are the majority of the systems described in the current literature. However, the selection of droop coefficients introduces a trade-off between power sharing and voltage regulation, which is also strongly influenced by line impedances [10]–[12]. In order to correct power sharing mismatches and dc bus voltage deviation, the secondary control level gathers information concerning local measurements of each converter, through a communication link, and provides means to modify primary level parameters that will lead to proportional power distribution and a regulated bus voltage. The secondary layer implementation can be either centralized or distributed. The centralized approach presents reduced reliability due to the existence of a single point of failure (SPoF), hence, the employment of distributed control schemes becomes a better solution [13]–[15].

Voltage deviation and power sharing corrections are mainly performed by adding a voltage shifting term to the droop controller of the power converters. In [13], a centralized controller senses the dc bus voltage and determines a voltage correction term that is broadcasted to all converters, in order to compensate the voltage deviation. In [5], [11], [16], [17], distributed control is employed, however, each converter needs to exchange information with every other converter in the microgrid, in order to be able to calculate the average values of the dc bus voltage and load current and then determine the appropriate voltage shifting quantity. Sparse communication network and consensus-based algorithm are described in [18]–[29], which only require information exchange between neighboring converters to converge to proper voltage regulation and power sharing, thus, improving the robustness of the microgrid control to communication failures and enabling the use of low bandwidth communication (LBC).

In terms of power sharing correction, voltage shifting approaches cannot change the output impedance of the power converters, hence, in order to compensate line impedance mismatches, the voltage shifting term must be constantly updated. Another possibility is to adjust the droop slope, aiming at mitigating the line impedance influence. Hybrid control strategies, which uses voltage shifting for dc bus voltage restoration and droop slope adjustment for power sharing correction, have been proposed in [30]–[32]. In [30], the converters exchange their droop resistance, output current and output voltage information and each of them computes the average value of these three parameters, using it to feed three separate compensators that will generate the voltage shifting action and adapt the converter droop resistance. The need for one converter to establish a communication with all the others is a drawback of this approach, since large microgrids can demand costly high bandwidth communication links and large data processing. In [31], [32], the hybrid structure is achieved through sparse communication and cooperative control, which improves the expandability of the system and resiliency against communication failures. However, the dc bus voltage deviation correction is dependent on a voltage observer structure, which estimates the dc bus average voltage that will be compensated.

In [33] a decentralized voltage restoration strategy is proposed for a hybrid energy storage system composed of one battery unit and one supercapacitor unit, both connected by

interfacing converters. In this strategy, the supercapacitor unit only responds to load variations, while the battery deals with the load power demand in steady state, therefore the dc link voltage is regulated by the battery alone, which allows a voltage shifting compensation to be added to the unit's voltage droop control reference and ensures a regulated dc voltage in steady state. However, the behavior of the proposed strategy in a scenario with multiple converters and under the influence of non negligible line impedances is not fully explored or validated. In deed, the simple expansion of this strategy to multiple paralleled converters will lead to high circulating currents between them, hence a coordinated current sharing strategy is mandatory, however, no discussions concerning the criteria to integrate the decentralized voltage restoration action with current sharing techniques are provided.

This paper proposes a secondary level strategy which uses distributed control to promote proportional power sharing and a decentralized voltage shifting action to restore the dc bus voltage. The existence of the power sharing action prevents high circulating currents to build up between converters in steady state and also compensates the average dc bus voltage errors introduced by the line impedances. A comprehensive design procedure and performance analysis is also provided. In the proposed method, a sparse communication network is employed where each converter exchanges its output power information with its neighbors through a LBC and uses the received data to tune its droop coefficient, compensating line impedance mismatches and leading to proportional power sharing. Once the power sharing correction is achieved, each converter employs only local information to generate a voltage shifting term, which mitigates the dc bus voltage deviation introduced by the droop control. This strategy reduces the information traffic and improves system reliability. Moreover, voltage restoration has shown to be more robust, being disturbed only by changes in the equivalent line impedances, i.e., if load variations do not alter the line impedances seen by the converters, voltage regulation is ensured even during severe communication failures. It also has shown to provide small voltage oscillations under fairly high communication delays, as confirmed by simulation results. Table I offers a comparison between features of secondary control structures found in literature and the proposed strategy.

This work is outlined as follows: Section II analyzes power and current sharing problems in dc microgrids. Section III presents the proposed secondary level control technique. Section IV analyzes the influence of the proposed technique on the system voltage stability. Section V and VI present the simulation and experimental results, respectively, and Section VII shows the paper conclusions.

II. DISCUSSION ON CURRENT AND POWER SHARING PROBLEMS IN DC MICROGRIDS

The following discussion will consider the simplified model of a dc microgrid presented in Fig. 2, which is composed by two converters (*Conv-1* and *Conv-2*), represented by their steady state Thevenin equivalent circuit, line resistances (r_1 and r_2) and a resistive load $R_{\mu G}$. V_{o1}^* and V_{o2}^* refer to the nominal reference voltage of *Conv-1* and *Conv-2*, R_{d1} and R_{d2} are the droop coefficients and $v_{\mu G}$ is the dc bus voltage

TABLE I
COMPARISON OF SECONDARY CONTROLLERS FOR A DC MICROGRID

| Literature proposal | Shared information | Communication among converters | Power/current sharing correction | Voltage restoration |
|--|---|--------------------------------|----------------------------------|---------------------|
| Lu <i>et al.</i> [4] | Voltage, Current | All | Voltage shifting | Distributed |
| Dam and Lee [16] | Voltage, Power | All | Voltage shifting | Distributed |
| Anand <i>et al.</i> [17] | Current | All | Voltage shifting | None |
| Xu <i>et al.</i> [33] | None | None | None | Decentralized |
| Meng <i>et al.</i> [18], Zhang <i>et al.</i> [21], Chen <i>et al.</i> [22], Mumtaz <i>et al.</i> [25], Pullaguram <i>et al.</i> [26] | Voltage, Current | Neighbors | Voltage shifting | Distributed |
| Wang <i>et al.</i> [19] | Voltage, Compensating term | Neighbors | Voltage shifting | Distributed |
| Moayedi and Davoudi [24] | Voltage, Incremental cost | Neighbors | Voltage shifting | Distributed |
| Sahoo and Mishra [28] | Voltage, Voltage dynamic averaging, Current | Neighbors | Voltage shifting | Distributed |
| Wang <i>et al.</i> [30] | Voltage, Droop coefficient, Current | All | droop-adjustment | Distributed |
| Nasirian <i>et al.</i> [31], Zaery <i>et al.</i> [32] | Voltage, Current | Neighbors | droop-adjustment | Distributed |
| Proposed technique | Power | Neighbors | droop-adjustment | Decentralized |

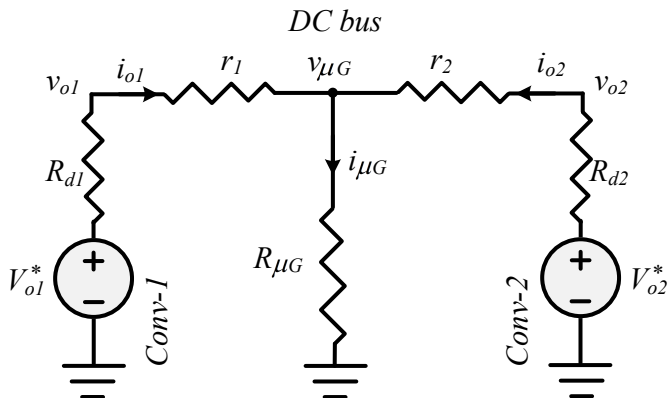


Fig. 2. Simplified model of a dc microgrid

The output current and power of the converters are expressed in (1) and (2), respectively.

$$i_{o1} = \frac{V_{o1}^* - v_{\mu G}}{R_{d1} + r_1} \quad (1)$$

$$i_{o2} = \frac{V_{o2}^* - v_{\mu G}}{R_{d2} + r_2}$$

$$P_1 = v_{\mu G} i_{o1} + r_1 i_{o1}^2 \quad (2)$$

$$P_2 = v_{\mu G} i_{o2} + r_2 i_{o2}^2$$

It can be noticed that if *Conv-1* and *Conv-2* are equal, i.e., $V_{o1}^* = V_{o2}^*$ and $R_{d1} = R_{d2}$, current ($i_{o1} = i_{o2}$) and power sharing ($P_1 = P_2$) can be achieved only if $r_1 = r_2$. In case of $r_1 \neq r_2$, converter equality will lead to unbalanced output current and power. In this case, current sharing can be achieved if $R_{d1} \neq R_{d2}$ and/or $V_{o1}^* \neq V_{o2}^*$, but concomitant power sharing would not be possible. Output power imbalance between converters can be an important issue in some applications, e.g., ESC in island mode operating, where power sharing mismatch leads to unequalized State-of-Charge (SoC). Therefore, considering that unequal line resistances will certainly be present in a real microgrid, ensuring power sharing over current sharing seems to be the right alternative.

From (1), it can be shown that in any circumstance

$$\frac{i_{o1}}{i_{o2}} = \frac{R_{d2} + r_2}{R_{d1} + r_1}, \quad (3)$$

whereas (2) can be manipulated into

$$\frac{P_1}{P_2} = \frac{i_{o1}}{i_{o2}} \left(\frac{v_{\mu G} + r_1 i_{o1}}{v_{\mu G} + r_2 i_{o2}} \right) = m_p, \quad (4)$$

where m_p is a desired power ratio between the two converters. Since $v_{\mu G} = R_{\mu G}(i_{o1} + i_{o2})$, the current ratio can also be defined, from (4), as

$$\frac{i_{o1}}{i_{o2}} = -a + \sqrt{b} = m_i \quad (5)$$

where m_i is the current ratio that enables m_p , and

$$a = \frac{(1 - m_p)}{2(1 + \frac{r_1}{R_{\mu G}})}$$

$$b = m_p \left(\frac{1 + \frac{r_2}{R_{\mu G}}}{1 + \frac{r_1}{R_{\mu G}}} \right) + \left[\frac{1 - m_p}{2(1 + \frac{r_1}{R_{\mu G}})} \right]^2$$

If a droop slope correction term (δR_{dj} , $j = 1, 2$) is added to the droop coefficient of each converter, it can be shown from (3) that

$$\frac{i_{o1}}{i_{o2}} = \frac{(R_{d2} + \delta R_{d2}) + r_2}{(R_{d1} + \delta R_{d1}) + r_1} \quad (6)$$

Therefore, there is a combination of δR_{d1} and δR_{d2} that enforces $i_{o1}/i_{o2} = m_i$, hence compensating the line impedance mismatch and ensuring proportional power sharing. It is noteworthy that an adequate m_i can also be found for generic loads, although in some cases, e.g., Constant Power Loads (CPL), an analytical solution as the one described in (5), which does not rely on converter parameters, might not exist.

III. PROPOSED HYBRID CONTROL METHOD

Fig. 3 shows the proposed control diagram. It is assumed that the microgrid comprises N converters sharing the main dc bus, where *Conv- j* ($j = 1, 2, \dots, N$) communicates with a set of neighboring converters N_j through a LBC link. At initialization of the control algorithm, *Conv- j* polls each *Conv- k* and registers its nominal droop coefficient R_{dk} , where $k \in N_j$. Afterwards, in each control cycle, determined by the communication sampling time τ_{LBC} , the communication

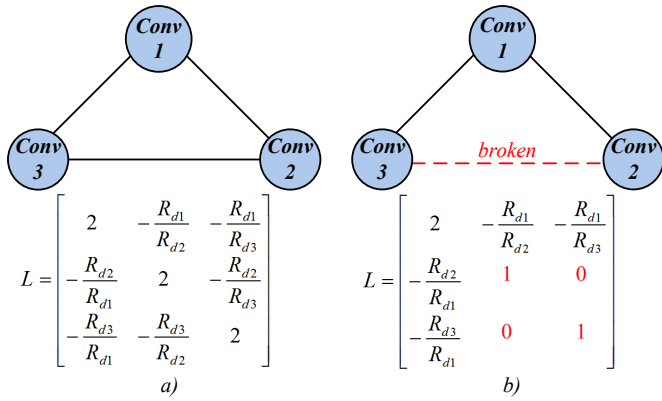


Fig. 5. Network topology

neighbors, otherwise $a_{jk} = 0$ [18]. From a system point of view, (14) can be expressed in vector form [35], [36]:

$$X(t+1) = WX(t) \quad (15)$$

where $X(t) = [x_1(t), x_2(t), \dots, x_N(t)]^T$ and W is the communication network weighting matrix, defined by [18]:

$$W = I - \epsilon L \quad (16)$$

$$L = \begin{bmatrix} \sum_{k \in N_1} a_{1k} & \dots & -a_{1N} \\ \vdots & \ddots & \vdots \\ -a_{1N} & \dots & \sum_{k \in N} a_{Nk} \end{bmatrix} \quad (17)$$

where I and L are the Identity and Laplacian matrices of the communication network, respectively. Hence, the states of all agents will converge to a consensus value [36]:

$$\lim_{t \rightarrow \infty} X(t) = \lim_{t \rightarrow \infty} W^t X(0) = \left(\frac{1}{N} \mathbf{1} \mathbf{1}^T \right) X(0) \quad (18)$$

where $\mathbf{1}$ is a vector with all the components equal to one and $X(0)$ are the initials states.

Considering (7) and the communication network topologies shown in Fig. 5, Fig. 5-a) presents the Laplacian matrix for a daisy chain topology, whereas Fig. 5-b) considers a situation where one link is broken. A constant weighting value $\epsilon = \tau_{LBC} / [(N+1)\tau_p]$ was adopted, corresponding to power time constant and following the ϵ definition methods discussed in [18], [36].

Considering $x_j(t) = R_{dj} + \delta R_{dj}(t) + r_j$, assuming $\delta R_{dj}(0) = 0$ and using the equations (15)-(18), it is obtained:

$$\lim_{t \rightarrow \infty} X(t) = \frac{1}{\sum_{j=1}^N R_j} \left(\begin{bmatrix} R_{d1} & \dots & 0 \\ \vdots & \ddots & \vdots \\ 0 & \dots & R_{dN} \end{bmatrix} [\mathbf{1}W] \right) X(0) \quad (19)$$

where $[\mathbf{1}] = \mathbf{1} \mathbf{1}^T$. Rewriting $x_j(t)$ to $\delta R_{dj}(t) = x_j(t) - R_{dj} - r_j$ and replacing it in $X(t)$ in (19), one obtains:

$$\lim_{t \rightarrow \infty} \delta R_d(t) = \left(\frac{1}{\sum_{j=1}^N R_j} \begin{bmatrix} R_{d1} & \dots & 0 \\ \vdots & \ddots & \vdots \\ 0 & \dots & R_{dN} \end{bmatrix} [\mathbf{1}W - [I]] \right) X(0) \quad (20)$$

and

$$\sum_{j=1}^N \delta R_{dj}(t) = 0 \quad (21)$$

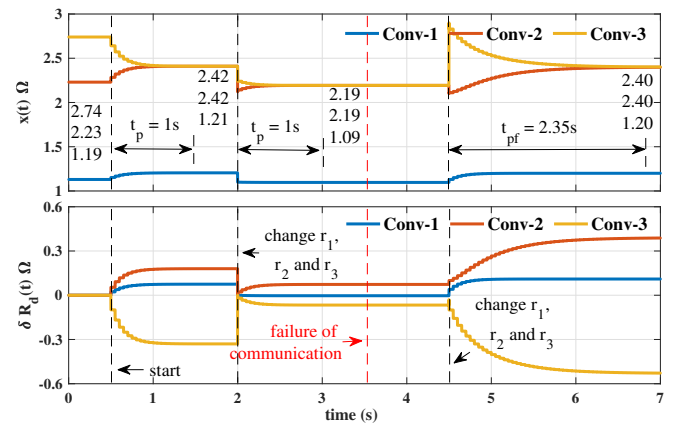


Fig. 6. Convergence of $\delta R_d(t)$

Assuming the simplified dc bus model of Fig. 2, with two equal converters, hence, $R_{d1} = R_{d2}$ and $r_1 \neq r_2$, (20) and (21) results in:

$$\delta R_{d1} = -\delta R_{d2} = \frac{r_2 - r_1}{2} \quad (22)$$

The average output voltage of the converters is expressed as (23). Substituting (22) in (11) and the result in (23), one can obtain (24). Since $(r_2 - r_1)/4 \ll 1$, then $v_{avg} \approx V_o^*$.

$$v_{avg} = \frac{v_{o1} + v_{o2}}{2} \quad (23)$$

$$v_{avg} = V_o^* - \frac{r_2 - r_1}{4} (i_{o1} - i_{o2}) \quad (24)$$

As an example, consider a dc microgrid with three converters in a daisy chain structure, as depicted in Fig. 5-a), where the droop coefficients are chosen so that the power ratio is 0.5:1:1, hence, $R_{d2} = R_{d3} = 2R_{d1} = 2\Omega$, the line resistances are $r_1 = 0.19\Omega$, $r_2 = 0.23\Omega$ and $r_3 = 0.74\Omega$ and $\tau_{LBC} = 50ms$, $\tau_p = 0.2$. Note that, since $r_j \ll R_{dj}$, power and current ratios are similar. Fig. 6 shows the convergence dynamic of $\delta R_d(t)$ and $x(t)$, under different conditions of the microgrid. The compensation action starts at $t = 0.5s$ and at $t = 2s$ a load modification changes the values of the equivalent line resistances to $r_1 = 0.1\Omega$, $r_2 = 0.12\Omega$ and $r_3 = 0.26$. In both circumstances, it can be observed that $x(t)$ converges to the specified power ratio with the same time interval t_p . In $t = 3.5s$ occurs a communication failure between Conv-2 and Conv-3, which does not affect the power ratio, since no alteration in line resistances took place during that event. Finally, at $t = 4.5s$ the line impedances change to $r_1 = 0.1\Omega$, $r_2 = 0.1\Omega$ and $r_3 = 0.9$ and once again convergence is achieved, however, it can be observed that if a communication failure occurs, the convergence time will be longer. The error in $x(t)$ decreases exponentially with a rate that is related to the eigenvalues ($\lambda(\cdot)$) of matrix L , thus, $\lambda(\cdot)$ determine the global dynamics [37]–[39]. In this sense, the broken link Laplacian, shown in Fig.5.b, presents a set of eigenvalues that will result in a convergence time $t_{pf} = 2.35t_p$, i.e., 2.35 times longer than the daisy chain communication structure.

B. Time delay on consensus-based algorithm

Dynamic consensus-based algorithm stability can be sensitive to time delays. According to [39], [40], considering uniform communication link delays $\tau_{jk} = \tau_d$, the consensus

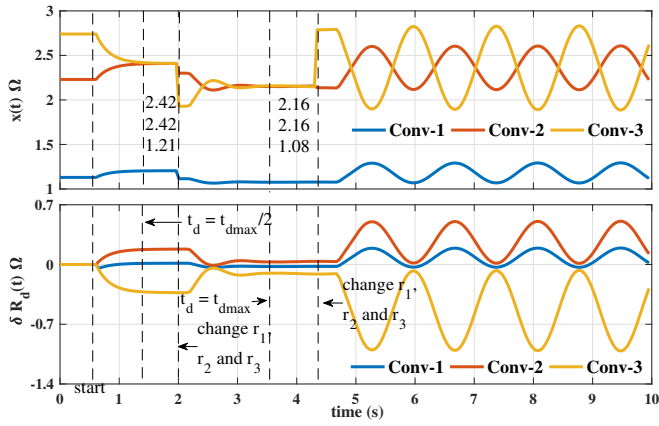


Fig. 7. Convergence of $\delta R_d(t)$ with time delay

algorithm converges if $\tau_d < \pi/2\lambda_N$, where λ_N is the largest eigenvalue of the matrix L . Since τ_d is inversely proportional to λ_N , then, conservatively, one can assume $\tau_{dmax} < \pi/2N$ as time delay limit, because λ_N will be lower than the order of matrix L . Moreover, for $\tau_d = \pi/2\lambda_N$ the system has a stable oscillatory solution with frequency $\omega = \lambda_N$ [39]. Therefore, the communication on large networks should be carefully designed to minimize time delays or to increase the maximum tolerable delay time, e.g., reducing the number of connections per node.

In order to illustrate the influence that large time delays can have on the microgrid behavior, the example described in the previous section was revisited, assuming a time delay (t_d) between the nodes. Fig. 7 shows the $\delta R_d(t)$ convergence considering the same parameters of $R_{d1,2,3}$ and $r_{1,2,3}$ in Fig. 6. At $t = 0.5s$ the control is enabled with $t_d = 0$ and at instants $t = 1.2s$ and $t = 3.5s$, the time delays are increased to $t_{dmax}/2$ and t_{dmax} , respectively. Notice that, for $t_d < t_{dmax}$, the system converges asymptotically, however, the time delay lowers the transient response damping. However, when $t_d = t_{dmax}$, the transient response becomes marginally stable, oscillating around the consensus values.

IV. STABILITY ANALYSIS

From the dc microgrid model in Fig. 2, the output current of the converters can be expressed as:

$$\begin{aligned} i_{o1} &= \alpha_1 v_{o1} - \beta v_{o2} \\ i_{o2} &= \alpha_2 v_{o2} - \beta v_{o1} \end{aligned} \quad (25)$$

where

$$\begin{aligned} \alpha_1 &= \frac{r_2 + R_{\mu G}}{r_1 r_2 + R_{\mu G}(r_1 + r_2)} \\ \alpha_2 &= \frac{r_1 + R_{\mu G}}{r_1 r_2 + R_{\mu G}(r_1 + r_2)} \\ \beta &= \frac{R_{\mu G}}{r_1 r_2 + R_{\mu G}(r_1 + r_2)}. \end{aligned} \quad (26)$$

The closed-loop control diagram of *Conv-1* is shown in Fig. 8. Assuming that τ_{LBC} is much greater than the converter response time, δv_{o1} and δR_{d1} can be seen as perturbations on the voltage reference and the droop coefficient, respectively. The communication delay is represented by $e^{-\tau_d s}$ and a second-order Padé approximation is used to model the time

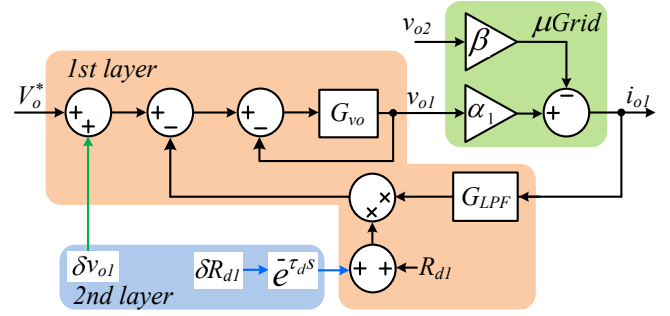


Fig. 8. Control diagram for stability analysis

TABLE II
STABILITY ANALYSIS PARAMETERS

| Item | Symbol | Value |
|-------------------------------------|--------------|-----------|
| Nominal voltage | V_o^* | 380V |
| Line impedance | $r_{1,2}$ | 0.1, 0.9Ω |
| Droop Coefficient | $R_{d1,2}$ | 2.3, 2.3Ω |
| Load resistance | $R_{\mu G}$ | 32.9Ω |
| Communication sampling | τ_{LBC} | 50ms |
| Communication delay | τ_d | 1ms |
| LPF cut-off frequency | f_c | 100Hz |
| Power sharing speed correction gain | K_P | 20 |
| Voltage speed correction gain | K_V | 2 |

delay. The closed-loop transfer function is expressed as [3], [4]:

$$G_{vo} = \frac{G_{PI}G_C}{1 + G_{PI}G_C} \quad (27)$$

where G_{PI} and G_C are the voltage loop PI compensator and the current loop transfer function, respectively. G_C can be represented as a delay unit [11]. Therefore, the output voltages of the converters can be defined as:

$$\begin{aligned} v_{o1} &= [V_o^* - i_{o1}G_{LPF}(R_{d1} + \delta R_{d1})]G_{vo} \\ v_{o2} &= [V_o^* - i_{o2}G_{LPF}(R_{d2} + \delta R_{d2})]G_{vo} \end{aligned} \quad (28)$$

where

$$\begin{aligned} G_{LPF} &= \frac{2\pi f_c}{s + 2\pi f_c} \\ \delta R_{d1} &= \frac{r_2 - r_1}{2} \\ \delta R_{d2} &= \frac{r_1 - r_2}{2} \end{aligned} \quad (29)$$

Combining (25)-(29) yields (30), which enables the assessment of the influence of parameter variation on stability.

$$\begin{aligned} \frac{v_{o1}}{V_o^*} &= \frac{G_{vo}}{1 + [\alpha_1 G_{LPF}(R_{d1} + \frac{r_2 - r_1}{2}) + 1]G_{vo}} \\ \frac{v_{o2}}{V_o^*} &= \frac{G_{vo}}{1 + [\alpha_2 G_{LPF}(R_{d3} + \frac{r_1 - r_2}{2}) + 1]G_{vo}} \end{aligned} \quad (30)$$

Fig. 9 presents the root loci of the dominant poles under variations on r_1 , R_{d1} , δR_{d1} and t_d . Table II describes the parameters employed in this analysis. Fig 9a shows the influence of the line impedance on the system closed-loop poles. The value of r_2 is fixed and r_1 was altered from 0.01Ω to R_{d1} , allowing the evaluation of $r_1 < r_2$ and $r_1 > r_2$. Fig. 9b shows the root locus for variations in R_{d1} , where R_{d1} vary from $0.1R_{d1}$ to $1.9R_{d1}$ whereas the value of R_{d2} is fixed. Fig.

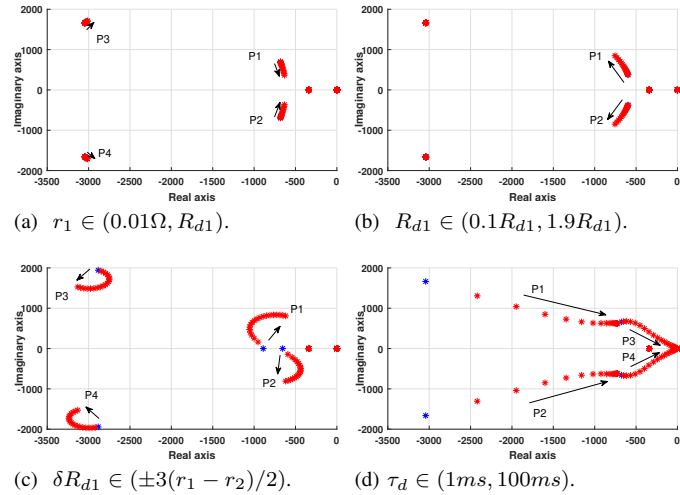


Fig. 9: Root loci of the closed-loop poles under parameter variation.

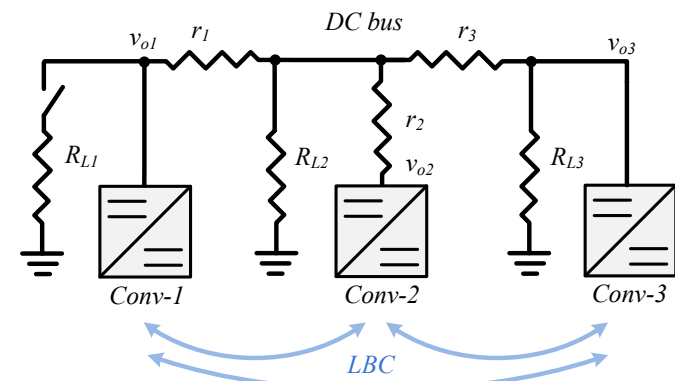


Fig. 10. DC microgrid in simulation

9c presents the root locus for variations in δR_{d1} , where δR_{d1} was varied from $-3(r_1 - r_2)/2$ to $-3(r_1 - r_2)/2$ and finally, Fig. 9d shows the variation in τ_d from $1ms$ to $100ms$. In all four situations only the higher frequency complex poles were affected by the parameter variation, with distinct trajectories. However, in all cases, in the considered parameter variation ranges, all dominant poles stayed in the LHS of the complex plan, thus, indicating that the system will remain stable. It is noteworthy that the time delay response is the more critical, since as the time delay approaches t_{dmax} , transient response damping is dramatically reduced with poles moving toward the imaginary axis.

V. SIMULATION RESULTS

In order to evaluate the performance of the proposed control, a microgrid with three converters, as illustrated in Fig. 10, was simulated in PLECS 4.1. Table III presents the parameters considered in this simulation study. A Dual Active Bridge (DAB) topology was considered for each converter, in order to hold compatibility with the available experimental setup.

Fig. 11 shows the control performance without load perturbation. At the beginning of the simulation, only droop control is active, leading to a $376.4V$ average dc bus voltage and unbalanced power between converters, where $P_1 = 0.88kW$, $P_2 = 0.56kW$ and $P_3 = 0.74kW$. In $t = 1s$ the secondary control is enabled. Afterwards, accurate proportional power sharing is achieved in $t_p = 1s$, whereas the average dc bus

TABLE III
SIMULATION PARAMETERS

| Item | Symbol | Value |
|-------------------------------------|----------------|-------------------------|
| Nominal Voltage | V_O^* | 380V |
| Line impedance | $r_{1,2,3}$ | 0.9, 0.9, 0.1 Ω |
| Droop Coefficient | $R_{d1,2,3}$ | 1.15, 2.3, 2.3 Ω |
| Rated power of the converters | $P_{1,2,3}$ | 3.2, 1.6, 1.6kW |
| Loads | $R_{L1,L2,L3}$ | 65.4, 133, 133 Ω |
| Communication sampling time | τ_{LBC} | 50ms |
| Power sharing speed correction gain | K_P | 20 |
| Voltage speed correction gain | K_V | 2 |
| Switching frequency | f_{sw} | 15kHz |
| DAB transformer turns ratio | n | 7.9 : 1 |
| PI voltage controller | PI | $k_p = 1.8, k_i = 276$ |
| PI current controller | PI | $k_p = 0.3, k_i = 20$ |
| Current and voltage sensor gains | $H_{i,v}$ | 0.1, 0.01 |

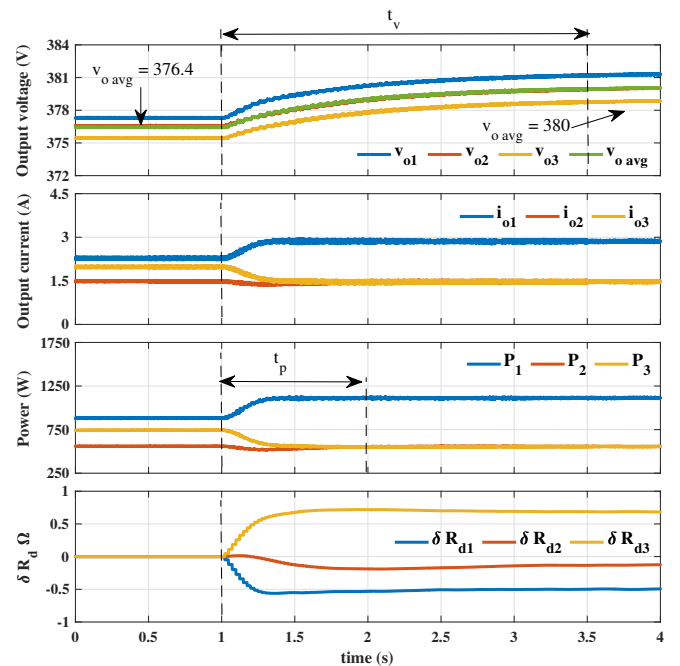


Fig. 11. System behavior up to complete dc bus voltage restoration

voltage converges to $380V$ in $t_v = 2.5s$, confirming that the simplification adopted to solve (9) is plausible. The droop correction terms converge to $\delta R_{d1} = -0.512\Omega$, $\delta R_{d2} = -0.142\Omega$ and $\delta R_{d3} = 0.654\Omega$, thus, $\delta R_{d1} + \delta R_{d2} + \delta R_{d3} = 0$. Moreover the output power of the converters converge to $P_1 = 1.1kW$, $P_2 = 0.55kW$ and $P_3 = 0.55kW$, whereas the output currents are $i_{o1} = 2.82A$, $i_{o2} = 1.46A$ and $i_{o3} = 1.45A$, showing a small imbalance between current and power ratios, as also expected.

Fig. 12 shows system behavior against load perturbation and communication failures. The system initial condition is equal to the final values of Fig. 11. In $t = 5.5s$ (event A), load R_{L2} is connected to the dc bus, disturbing the output voltages of the power converters. However, the equivalent line resistances are not affected, which does not introduces new power sharing mismatches. Therefore, all converters proportionally increase their output power not altering the steady state value of the droop correction terms, while the decentralized voltage correction gradually regulates the dc bus voltage. In $t = 7.5s$

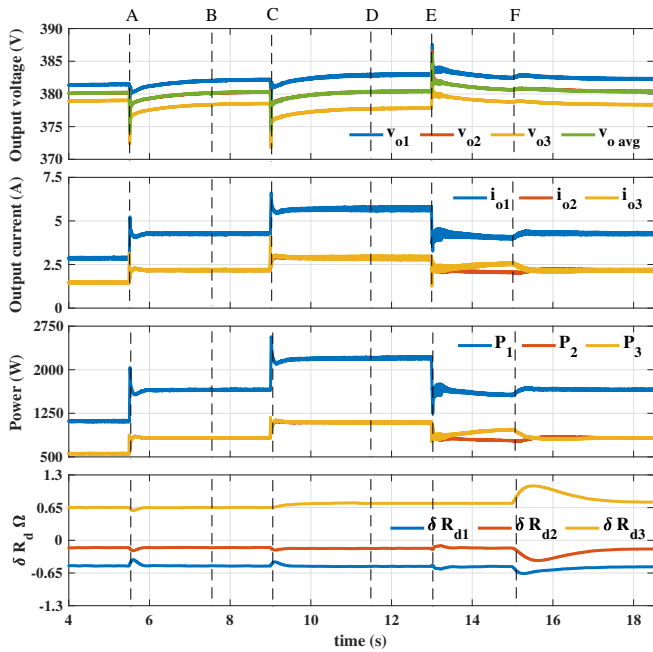


Fig. 12. System behavior under load perturbation and communication failures

(B), there is a communication failure between *Conv-1* and *Conv-3*, however, since there was no load and line resistance alterations, the correction of voltage deviation and power sharing were preserved. In $t = 9s$ (C), R_{L3} is connected to the dc bus, causing a new disturbance on the output voltages and an alteration on equivalent line impedances, hence, the secondary control calculates new values of δR_d for ensuring power sharing. In this case, convergence occurred in $t_p = 0.1s$.

At $t = 11.5s$ (D), a new communication failure occurs, now between *Conv-2* and *Conv-3*, which leaves *Conv-3* isolated from the other converters. Since it receives no data from the remainder converters, voltage deviation correction is halted, holding the last δv_{o3} and δR_{d3} values. Accurate power sharing will be ensured, as long as there are no equivalent line impedance changes. In $t = 13s$ (E), R_{L2} is disconnected from the dc bus, perturbing the dc bus voltage and modifying the equivalent line impedance. It can be observed that the power ratio between *Conv-1* and *Conv-2* is conserved, regardless of *Conv-3*. The voltage deviation correction performed by converters 1 and 2 is still active, which reduces the dc bus voltage error, but increases the difference between the output currents i_{o2} and i_{o3} . The droop correction terms converged to $\delta R_{d1} = -0.522\Omega$, $\delta R_{d2} = -0.154\Omega$ and $\delta R_{d3} = 0.735\Omega$. Finally, at $t = 15s$ (F), the communication with *Conv-3* is restored and as a result the accurate power sharing among the three converters is restored as well.

In order to assess the performance of the proposed technique with different load types and in the presense of significant communication delay, a simulation was assembled where R_{L1} and R_{L3} were supplanted by CPLs of 2.2kW and 1.1kW, respectively, the δR_d value was limited from -1.2Ω up to 1.2Ω and a fixed time delay was included in each communication link. The same scenario was simulated for three time delays: $t_d = 0$, $t_d = 53ms = \tau_{dmax}/10$ and $\tau_d = 530ms \approx t_{dmax}$ and the results are presented in Fig. 13. At the beginning only R_{L1} is supplied and the system operates with $\hat{V}_O = 376V$

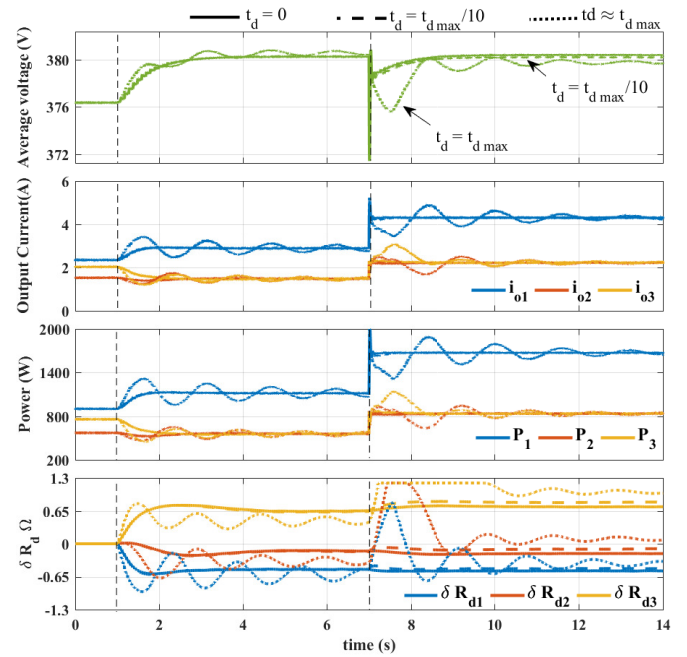


Fig. 13. DC bus with CPL and considering time delays

$P_1 = 0.9kW$, $P_2 = 0.76kW$ and $P_3 = 0.57kW$. At $t = 1s$, the secondary control is enabled. It can be noticed that for $t_d \leq t_{dmax}/10$ no significant difference in the system performance is observed and the same power and output current values were obtained: $P_1 = 1.1kW$, $P_2 = 0.55kW$, $P_3 = 0.55kW$, $i_{o1} = 2.9A$, $i_{o2} = 1.43A$ and $i_{o3} = 1.42A$. On the other hand, $t_d \approx t_{dmax}$ interferes with power sharing and δR_d values become more oscillatory what is reflected to the converters' output power, current and voltage. It is important to mention that this scenario is extremely unrealistic for a 3 node system, since 530ms exceeds the reported communication delay found in most implementations. Anyhow, the system has show to be tolerant to moderate communication delays ($t_d < t_{dmax}$). The average voltage, even under severe time delay, remained close to the reference value (380V) with small ripple. In $t = 7s$, R_{L3} is connected to the dc bus. Notice that with $t_d = t_{dmax}$, δR_{d2} and δR_{d3} saturate for a few seconds. Nonetheless, the output powers oscillate around the $P_1 = 1.68kW$, $P_2 = 0.84kW$ and $P_3 = 0.84kW$ and achieve consensus, since the increase in the load power shifts the close loop poles away from the imaginary axis.

At last, Fig. 14 shows the behavior of the output voltage v_o , power P and δR_d of *Conv-1*, assuming different values for K_P in all three converters. The secondary control is enabled at $t = 0.5s$ and it can be observed that the convergence of the voltage deviation correction is not affected by K_P . For $K_P > 1/\tau_{LBC}$ the system response damping is reduced leading to oscillations on the output voltage as well as in δR_d . The system does not become unstable, nevertheless.

VI. EXPERIMENTAL RESULTS

The proposed control strategy was experimentally validated through a dc microgrid setup with a 3.2 kW BIC and 2x 1.6 kW DAB converters, as depicted in Fig 15. *Conv-1* is a bidirectional utility interface converter, implemented by two full-bridge stages in which the dc/dc stage performs the droop control as proposed in this paper and the ac/dc stage controls

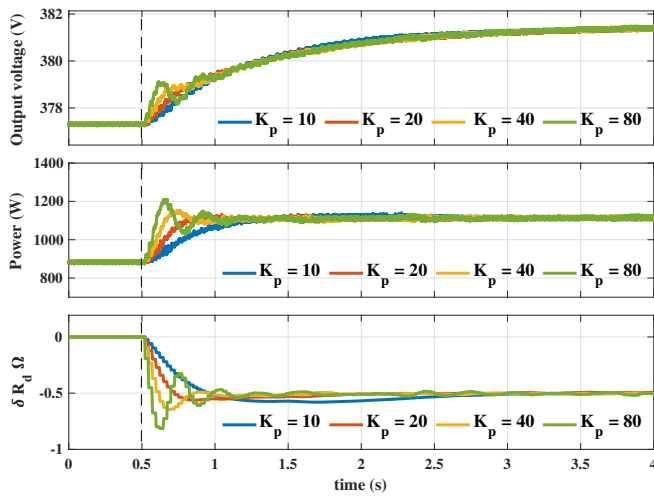


Fig. 14. Results of *Conv-1* to different values of K_P

the injected utility current in order to regulate the inner dc link at 550V. The dc link capacitance is designed so the dynamics of both stages are decoupled, therefore, the ac/dc control diagram will be omitted here. *Conv-2* and *Conv-3* are DAB converters that interface the dc bus to two battery banks. The control system, in each converter, was implemented on a TMS320F28335 Texas Instruments DSP and a 500 kbps CAN 2.0 communication network was employed to exchange information among converters. A Raspberry Pi 3 is also attached to the CAN network and was used as a datalogger. The converter parameters are the ones described in Table III.

The results without load perturbation are shown in Fig. 16. For $t < 1s$, the output power of *Conv-1*, *Conv-2* and *Conv-3* are $0.9kW$, $0.58kW$ and $0.77kW$, respectively, and the average voltage $v_{oavg} = 376.1V$. In $t = 1s$ the secondary control is enabled. The power sharing convergence time is observed to be $t_p \approx 1.2s$ and the voltage deviation correction occurred in $t_v = 2.5s$, once again the simplification adopted in (9) is confirmed. The output power of *Conv-1*, *Conv-2* and *Conv-3* converged to $1.16kW$, $0.58kW$ and $0.58kW$, respectively. It can be observed that with the secondary control the power sharing is proportional to the respective designed capacities of the converters. The droop correction terms are $\delta R_{d1} = -0.469\Omega$, $\delta R_{d2} = -0.172\Omega$ and $\delta R_{d3} = 0.499\Omega$, but $\delta R_{d1} + \delta R_{d2} + \delta R_{d3} = -0.142\Omega$, this can be explained by measurement inaccuracies. The output currents are $i_{o1} = 2.98A$, $i_{o2} = 1.52A$ and $i_{o3} = 1.51A$

Fig. 17 shows the results for a series of load perturbations occurring right after the previous experiment. Load R_{L2} is connect to the dc bus at $t = 5.5s$ (A). A priori, this load would not cause changes in the equivalent line impedances, however, there are resistances that were not modelled, e.g., connectors, thus a perturbation in the line impedance is sensed by *Conv-3*, which changes δR_{d3} from 0.478Ω to 0.243Ω in $t_p = 0.9s$.

A loss of communication occurs at $t = 7.4s$ (B) between *Conv-1* and *Conv-3*, which does not influence the power sharing and voltage regulation. At $t = 9s$ (C), load R_{L3} is connected to the dc bus. Power sharing convergence is achieved in $t_p = 0.9s$. It can be observed that this event did not provoke significant alterations in the values of the droop correction terms. The communication between *Conv-1* and *Conv-3* is restored at $t = 11.4s$ (D) and in $t = 13s$

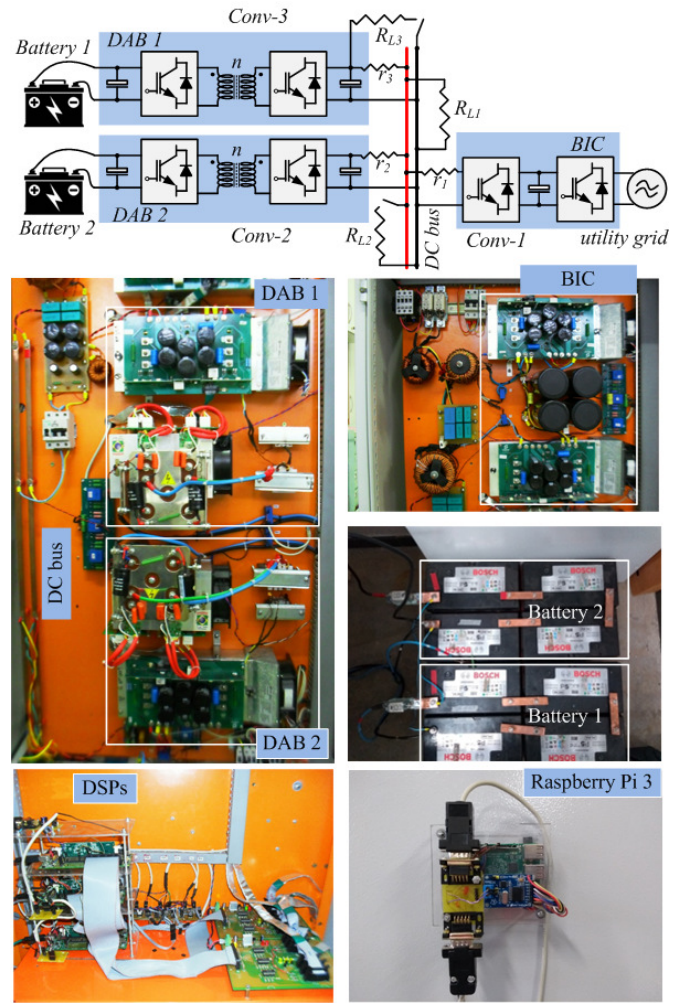


Fig. 15. DC microgrid experimental

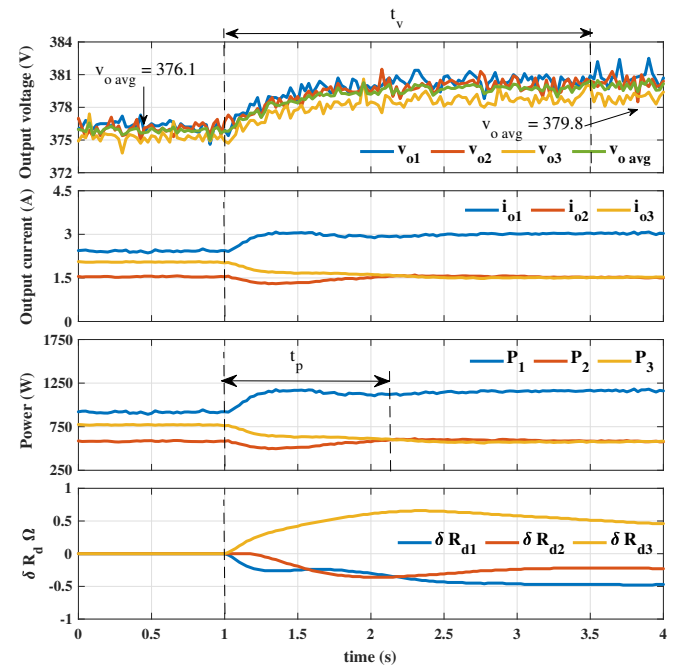


Fig. 16. Experimental results up to complete dc bus voltage restoration

(E) the load R_{L2} is disconnected from the dc bus. Once again, it can be observed that the proposed technique ensures proportional power sharing and that the voltage deviation

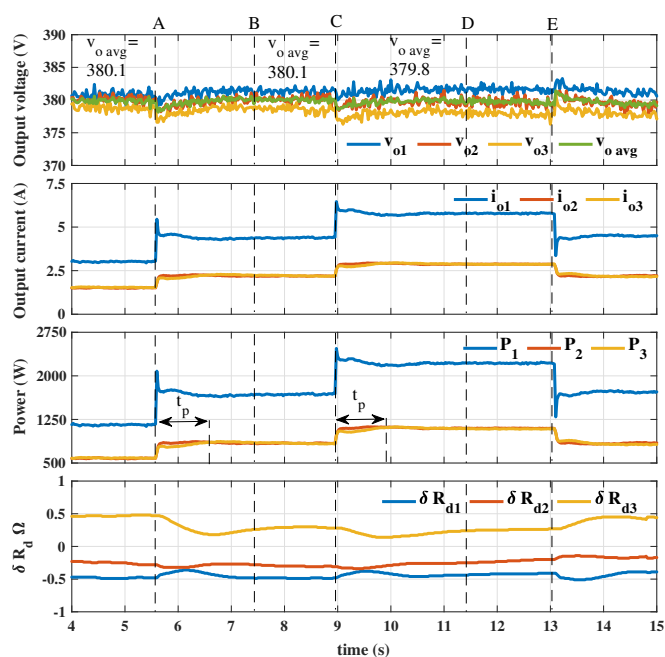


Fig. 17. Experimental results considering load perturbations and communication failure

correction was successful in regulating the dc bus average voltage to $v_{oavg} \approx V^*$. It can also be observed that the intrinsic time delay present in the CAN 2.0 communication link did not interfere with the system behavior.

VII. CONCLUSION

In this paper, a secondary level control strategy was proposed for achieving accurate power sharing and dc bus voltage restoration for dc microgrids. The proposed technique uses a distributed consensus-based algorithm to define a proper droop coefficient adjustment term that will be added to the droop controller of the power converters connected to the main dc bus of a microgrid, in order to compensate the influence of line impedance mismatches and promote accurate proportional power sharing. The algorithm relies solely on output power information exchanged between neighboring converters through a low bandwidth communication network. If the communications fails, but one neighbor is still communicating, power sharing is ensured. Voltage deviation correction is achieved by a decentralized action, which generates a voltage shifting term to be added to the converter voltage reference through an accumulator that compensates the voltage drop introduced by the converter droop coefficient. The strategy has shown to be stable under different parameter variations and robust to some communication failure events and moderate time delays. The performance of the proposed method was validated experimentally, showing a robust strategy able to reach proportional power sharing and dc bus regulation with low communication traffic, resiliency to communication failures and simplicity.

REFERENCES

[1] R. H. Lasseter, A. A. Akhil, C. Marnay, J. Stephens, J. E. Dagle, R. T. Guttromson, A. S. Meliopoulos, R. J. Yinger, and J. H. Eto, "Integration of distributed energy resources: The certs microgrid concept," CERTS, Tech. Rep., 10/2003 2003.

[2] J. M. Guerrero, J. C. Vasquez, J. Matas, M. Castilla, and L. G. de Vicuna, "Control strategy for flexible microgrid based on parallel line-interactive ups systems," *IEEE Transactions on Industrial Electronics*, vol. 56, no. 3, pp. 726–736, March 2009.

[3] K. D. Hoang and H. Lee, "Accurate power sharing with balanced battery state of charge in distributed dc microgrid," *IEEE Transactions on Industrial Electronics*, vol. 66, no. 3, pp. 1883–1893, March 2019.

[4] X. Lu, J. M. Guerrero, K. Sun, and J. C. Vasquez, "An improved droop control method for dc microgrids based on low bandwidth communication with dc bus voltage restoration and enhanced current sharing accuracy," *IEEE Transactions on Power Electronics*, vol. 29, no. 4, pp. 1800–1812, April 2014.

[5] P. Huang, P. Liu, W. Xiao, and M. S. E. Moursi, "A novel droop-based average voltage sharing control strategy for dc microgrids," *IEEE Transactions on Smart Grid*, vol. 6, no. 3, pp. 1096–1106, May 2015.

[6] J. Banda and K. Siri, "Improved central-limit control for parallel-operation of dc-dc power converters," in *Proceedings of PESC '95 - Power Electronics Specialist Conference*, vol. 2, June 1995, pp. 1104–1110 vol.2.

[7] J. Rajagopalan, K. Xing, Y. Guo, F. C. Lee, and B. Manners, "Modeling and dynamic analysis of paralleled dc/dc converters with master-slave current sharing control," in *Proceedings of Applied Power Electronics Conference. APEC '96*, vol. 2, March 1996, pp. 678–684 vol.2.

[8] X. Sun, Y.-S. Lee, and D. Xu, "Modeling, analysis, and implementation of parallel multi-inverter systems with instantaneous average-current-sharing scheme," *IEEE Transactions on Power Electronics*, vol. 18, no. 3, pp. 844–856, May 2003.

[9] R. Pradhan, M. Chirayath, and S. Thale, "Coordinated control strategy for a dc microgrid with low bandwidth communication," in *2016 IEEE International Conference on Power Electronics, Drives and Energy Systems (PEDES)*, Dec 2016, pp. 1–6.

[10] J. M. Guerrero, J. C. Vasquez, J. Matas, J. L. Sosa, and L. G. de Vicuna, "Parallel operation of uninterruptible power supply systems in microgrids," in *2007 European Conference on Power Electronics and Applications*, Sept 2007, pp. 1–9.

[11] X. Lu, J. M. Guerrero, K. Sun, J. C. Vasquez, R. Teodorescu, and L. Huang, "Hierarchical control of parallel ac-dc converter interfaces for hybrid microgrids," *IEEE Transactions on Smart Grid*, vol. 5, no. 2, pp. 683–692, March 2014.

[12] C. Jin, J. Wang, and P. Wang, "Coordinated secondary control for autonomous hybrid three-port ac/dc/ds microgrid," *CSEE Journal of Power and Energy Systems*, vol. 4, no. 1, pp. 1–10, March 2018.

[13] J. M. Guerrero, J. C. Vasquez, J. Matas, L. G. de Vicuna, and M. Castilla, "Hierarchical control of droop-controlled ac and dc microgrids—a general approach toward standardization," *IEEE Transactions on Industrial Electronics*, vol. 58, no. 1, pp. 158–172, Jan 2011.

[14] T. Dragičević, J. M. Guerrero, J. C. Vasquez, and D. Škrlec, "Supervisory control of an adaptive-droop regulated dc microgrid with battery management capability," *IEEE Transactions on Power Electronics*, vol. 29, no. 2, pp. 695–706, Feb 2014.

[15] J. Xiao, P. Wang, and L. Setyawan, "Hierarchical control of hybrid energy storage system in dc microgrids," *IEEE Transactions on Industrial Electronics*, vol. 62, no. 8, pp. 4915–4924, Aug 2015.

[16] D. Dam and H. Lee, "A power distributed control method for proportional load power sharing and bus voltage restoration in a dc microgrid," *IEEE Transactions on Industry Applications*, vol. 54, no. 4, pp. 3616–3625, July 2018.

[17] S. Anand, B. G. Fernandes, and J. Guerrero, "Distributed control to ensure proportional load sharing and improve voltage regulation in low-voltage dc microgrids," *IEEE Transactions on Power Electronics*, vol. 28, no. 4, pp. 1900–1913, April 2013.

[18] L. Meng, T. Dragicevic, J. Roldán-Pérez, J. C. Vasquez, and J. M. Guerrero, "Modeling and sensitivity study of consensus algorithm-based distributed hierarchical control for dc microgrids," *IEEE Transactions on Smart Grid*, vol. 7, no. 3, pp. 1504–1515, May 2016.

[19] H. Wang, M. Han, J. M. Guerrero, J. C. Vasquez, and B. G. Teshager, "Distributed secondary and tertiary controls for v-droop-controlled-parallel dc-dc converters," *IET Generation, Transmission Distribution*, vol. 12, no. 7, pp. 1538–1546, 2018.

[20] L. Guo, Z. Guo, X. Li, C. Wang, C. Hong, and Y. Zhang, "Consensus-based distributed coordinated control for islanded dc microgrids," in *2017 IEEE Power Energy Society General Meeting*, July 2017, pp. 1–5.

[21] X. Zhang, M. Dong, and J. Ou, "A distributed cooperative control strategy based on consensus algorithm in dc microgrid," in *2018 13th IEEE Conference on Industrial Electronics and Applications (ICIEA)*, May 2018, pp. 243–248.

[22] F. Chen, R. Burgos, D. Boroyevich, E. Rodriguez-Diaz, L. Meng, J. C. Vasquez, and J. M. Guerrero, "Analysis and distributed control of power flow in dc microgrids to improve system efficiency," in *2016 4th International Symposium on Environmental Friendly Energies and Applications (EFEA)*, Sep. 2016, pp. 1–6.

- [23] D. O’Keeffe, S. Rivero, L. Albiol-Tendillo, and G. Lightbody, “Distributed hierarchical droop control of boost converters in dc microgrids,” in *2017 28th Irish Signals and Systems Conference (ISSC)*, June 2017, pp. 1–6.
- [24] S. Moayedi and A. Davoudi, “Unifying distributed dynamic optimization and control of islanded dc microgrids,” *IEEE Transactions on Power Electronics*, vol. 32, no. 3, pp. 2329–2346, March 2017.
- [25] M. A. Mumtaz, M. M. Khan, F. Xianghong, A. Karni, and M. T. Faiz, “An improved cooperative control method of dc microgrids based on finite gain controller,” in *2018 20th European Conference on Power Electronics and Applications (EPE’18 ECCE Europe)*, Sep. 2018, pp. P.1–P.9.
- [26] D. Pullaguram, S. Mishra, and N. Senroy, “Event-triggered communication based distributed control scheme for dc microgrid,” *IEEE Transactions on Power Systems*, vol. 33, no. 5, pp. 5583–5593, Sep. 2018.
- [27] M. Cucuzzella, S. Trip, C. De Persis, X. Cheng, A. Ferrara, and A. van der Schaft, “A robust consensus algorithm for current sharing and voltage regulation in dc microgrids,” *IEEE Transactions on Control Systems Technology*, pp. 1–13, 2018.
- [28] S. Sahoo and S. Mishra, “A distributed finite-time secondary average voltage regulation and current sharing controller for dc microgrids,” *IEEE Transactions on Smart Grid*, vol. 10, no. 1, pp. 282–292, Jan 2019.
- [29] J. Hu, J. Duan, H. Ma, and M. Chow, “Distributed adaptive droop control for optimal power dispatch in dc microgrid,” *IEEE Transactions on Industrial Electronics*, vol. 65, no. 1, pp. 778–789, Jan 2018.
- [30] P. Wang, X. Lu, X. Yang, W. Wang, and D. Xu, “An improved distributed secondary control method for dc microgrids with enhanced dynamic current sharing performance,” *IEEE Transactions on Power Electronics*, vol. 31, no. 9, pp. 6658–6673, Sept 2016.
- [31] V. Nasirian, A. Davoudi, F. L. Lewis, and J. M. Guerrero, “Distributed adaptive droop control for dc distribution systems,” *IEEE Transactions on Energy Conversion*, vol. 29, no. 4, pp. 944–956, Dec 2014.
- [32] M. Zaery, E. M. Ahmed, M. Orabi, and M. Youssef, “Operational cost reduction based on distributed adaptive droop control technique in dc microgrids,” in *2017 IEEE Energy Conversion Congress and Exposition (ECCE)*, Oct 2017, pp. 2638–2644.
- [33] Q. Xu, J. Xiao, X. Hu, P. Wang, and M. Y. Lee, “A decentralized power management strategy for hybrid energy storage system with autonomous bus voltage restoration and state-of-charge recovery,” *IEEE Transactions on Industrial Electronics*, vol. 64, no. 9, pp. 7098–7108, Sep. 2017.
- [34] *Introduction to the Controller Area Network (CAN)*, Texas Instruments, 8 2002, revised May 2016.
- [35] R. Olfati-Saber, J. A. Fax, and R. M. Murray, “Consensus and cooperation in networked multi-agent systems,” *Proceedings of the IEEE*, vol. 95, no. 1, pp. 215–233, Jan 2007.
- [36] L. Meng, T. Dragicevic, J. M. Guerrero, and J. C. Vasquez, “Dynamic consensus algorithm based distributed global efficiency optimization of a droop controlled dc microgrid,” in *2014 IEEE International Energy Conference (ENERGYCON)*, May 2014, pp. 1276–1283.
- [37] B. Van Scoy, R. A. Freeman, and K. M. Lynch, “Exploiting memory in dynamic average consensus,” in *2015 53rd Annual Allerton Conference on Communication, Control, and Computing (Allerton)*, Sep. 2015, pp. 258–265.
- [38] S. S. Kia, B. V. Scoy, J. Cortés, R. A. Freeman, K. M. Lynch, and S. Martínez, “Tutorial on dynamic average consensus: the problem, its applications, and the algorithms,” *CoRR*, vol. abs/1803.04628, 2018.
- [39] R. Olfati-Saber and R. M. Murray, “Consensus problems in networks of agents with switching topology and time-delays,” *IEEE Transactions on Automatic Control*, vol. 49, no. 9, pp. 1520–1533, Sep. 2004.
- [40] T. Morstyn, B. Hredzak, G. D. Demetriades, and V. G. Agelidis, “Unified distributed control for dc microgrid operating modes,” *IEEE Transactions on Power Systems*, vol. 31, no. 1, pp. 802–812, Jan 2016.